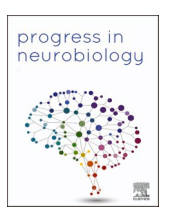
ELSEVIER

Contents lists available at ScienceDirect

Progress in Neurobiology

journal homepage: www.elsevier.com/locate/pneurobio





A tradeoff between efficiency and robustness in the hippocampal-neocortical memory network during human and rodent sleep

Michael A. Hahn ^{a,*}, Janna D. Lendner ^{a,b}, Matthias Anwander ^a, Katarina S.J. Slama ^c, Robert T. Knight ^c, Jack J. Lin ^{d,e}, Randolph F. Helfrich ^{a,*}

- ^a Hertie-Institute for Clinical Brain Research, University Medical Center Tübingen, Otfried-Müller Str. 27, Tübingen 72076, Germany
- b Department of Anesthesiology and Intensive Care Medicine, University Medical Center Tübingen, Hoppe-Seyler-Str 3, Tübingen 72076, Germany
- Department of Psychology and the Helen Wills Neuroscience Institute, UC Berkeley, 130 Barker Hall, Berkeley, CA 94720, USA
- ^d Department of Neurology, UC Davis, 3160 Folsom Blvd, Sacramento, CA 95816, USA
- e Center for Mind and Brain, UC Davis, 267 Cousteau Pl, Davis, CA 95618, USA

ARTICLE INFO

Keywords: Sleep Memory consolidation Population codes Cross-species Intracranial EEG

ABSTRACT

Sleep constitutes a brain state of disengagement from the external world that supports memory consolidation and restores cognitive resources. The precise mechanisms how sleep and its varied stages support information processing remain largely unknown. Synaptic scaling models imply that daytime learning accumulates neural information, which is then consolidated and downregulated during sleep. Currently, there is a lack of in-vivo data from humans and rodents that elucidate if, and how, sleep renormalizes information processing capacities. From an information-theoretical perspective, a consolidation process should entail a reduction in neural pattern variability over the course of a night. Here, in a cross-species intracranial study, we identify a tradeoff in the neural population code during sleep where information coding efficiency is higher in the neocortex than in hippocampal archicortex in humans than in rodents as well as during wakefulness compared to sleep. Critically, non-REM sleep selectively reduces information coding efficiency through pattern repetition in the neocortex in both species, indicating a transition to a more robust information coding regime. Conversely, the coding regime in the hippocampus remained consistent from wakefulness to non-REM sleep. These findings suggest that new information could be imprinted to the long-term mnemonic storage in the neocortex through pattern repetition during sleep. Lastly, our results show that task engagement increased coding efficiency, while medically-induced unconsciousness disrupted the population code. In sum, these findings suggest that neural pattern variability could constitute a fundamental principle underlying cognitive engagement and memory formation, while pattern repetition reflects robust coding, possibly underlying the consolidation process.

1. Introduction

Contemporary theories of sleep function posit that sleep reflects a brain state supporting memory consolidation, which involves the overnight regulation of neural activity at both synaptic and systems levels (Brodt et al., 2023; Lendner et al., 2023; Rasch and Born, 2013; Tononi and Cirelli, 2014). Far from being a passive state reflecting disengagement from the external world, recent theories highlight that sleep constitutes an active brain state that facilitates information processing (Brodt et al., 2023; Girardeau and Lopes-dos-Santos, 2021; Klinzing et al., 2019). At the systems-level, it has been suggested that mnemonic

information might be actively recapitulated through pattern repetition. This is exemplified by a process termed replay, which involves the periodic recurrence of neural firing patterns that were first present during encoding of new information (Foster, 2017; Ólafsdóttir et al., 2018). At the cellular level, pattern repetition might constitute a possible mechanism that promotes synaptic plasticity. Over the course of a night, repeated reactivation might strengthen relevant synapses, while irrelevant synapses are downscaled or 'pruned' (Tononi and Cirelli, 2014; Girardeau and Lopes-dos-Santos, 2021; Klinzing et al., 2019). From a Shannon information-theoretical perspective, neural information is reflected in patterns of neural activity, where high variability corresponds

E-mail addresses: michael.hahn@uni-tuebingen.de (M.A. Hahn), randolph.helfrich@gmail.com (R.F. Helfrich).

^{*} Correspondence to: Hertie-Institute for Clinical Brain Research, Center for Neurology, University Medical Center Tübingen, Otfried-Müller Str. 27, Tübingen 72076, Germany.

to a large amount of information (Luppi et al., 2024; Quian Quiroga and Panzeri, 2009; Timme and Lapish, 2018). Hence, the concepts of consolidation and downscaling entail that neural information content decreases over the course of the night, since information becomes repeated and condensed.

Pattern repetition is most commonly studied using single neuron recordings in the rodent hippocampus, as well as in putative human frontal cortex homologues (Ólafsdóttir et al., 2018; Euston et al., 2007; Peyrache et al., 2009). In humans, it remains challenging to record single unit activity from sufficiently large neuronal populations to reliably quantify recapitulated patterns. High-frequency band activity (HFA; 70 - 150 Hz) constitutes a viable proxy of multi-unit firing that can readily be obtained from macroelectrodes that are placed intracranially for localization of the seizure onset zone in pharmaco-resistant epilepsy patients (Leonard et al., 2024; Leszczyński et al., 2020; Parvizi and Kastner, 2018; Ray and Maunsell, 2011; Rich and Wallis, 2017). Importantly, the association between unit-firing and HFA has also been demonstrated in rodents using microelectrodes (Watson et al., 2018), providing a viable basis for cross-species comparisons. Pattern repetition had been described at the level of large-scale activity in humans (Jiang et al., 2017; Liu et al., 2019; Schwartenbeck et al., 2023); however, it remains unclear if the identified principles are comparable to the signatures previously identified in rodents. This gap in knowledge is due to the lack of comparative studies assessing human and rodent sleep using the same analytical methodology. In this study, we employed the information-theoretical approach of contrast entropy to quantify the neural information coding efficiency of HFA population signals in both species. Contrast entropy is defined as the ratio between the empirical entropy of a signal and its theoretical maximum, thereby reflecting its information coding efficiency.

We validated the analytical approach in simulations and then directly compared intracranial multi-site recordings from the hippocampus (HC; and adjacent structures in the medial temporal lobe; MTL) as well as from the medial and orbitofrontal cortex (mPFC/OFC) in rodents and humans during sleep. Moreover, we also included recordings from the human dorsolateral PFC (dlPFC), which is commonly considered the key structure underlying human cognitive abilities and which does not have clear homologue in rodents. We hypothesized that (1) neural efficiency should be higher in humans than in rodents, possibly reflecting the superior cognitive and mnemonic abilities. In addition, we reasoned that (2) neural efficiency should be higher in the frontal cortex as compared to the hippocampus. We predicted that (3) neural efficiency is lower during sleep, since neural patterns are replayed, especially during NREM sleep. We reasoned that recapitulation during sleep might support overnight consolidation. Hence, (4) we expected that information coding efficiency decreases over the course of the night. If the identified neural patterns are behaviorally relevant, then (5) neural efficiency should increase during cognitive engagement and (6) decrease in states of unconsciousness.

2. RESULTS

We assessed neural population information coding efficiency in nineteen human patients with pharmacologically intractable epilepsy (Helfrich et al., 2019) and eight Long Evans rats (Watson et al., 2018, 2016a) (for sleep characteristics see Table S1 & S2). In humans (Fig. 1A), electrode coverage encompassed the dorsolateral prefrontal cortex (dlPFC, N = 170), medial prefrontal cortex (mPFC, N = 134), orbitofrontal cortex (OFC, N = 62) and medial temporal lobe (MTL, N = 172) including contacts in the Hippocampus (HC, N = 124). All contacts with epileptic activity were excluded (Helfrich et al., 2019; Gelinas et al., 2016). We also leveraged rodent recordings (Fig. 1B; Watson et al., 2018) with comparable electrode coverage in mPFC (N = 718), OFC (N = 240) and HC (N = 104). We investigated sleep recordings in both species (Fig. 1C/D, top) to ensure a comparable brain state where a sufficient amount of data was available (Human: subset of 16 recording

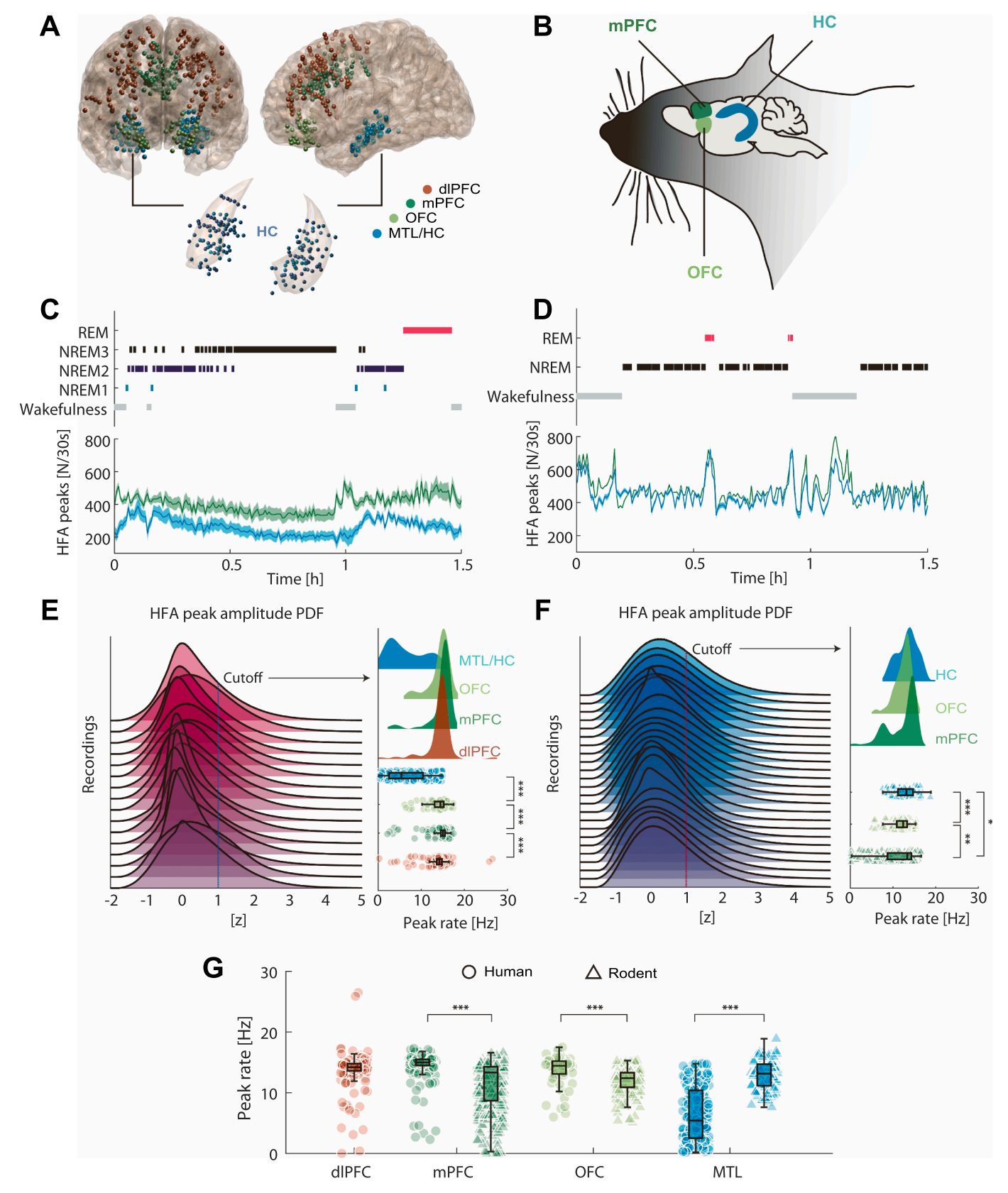
sessions with concurrent coverage in all regions-of-interest, $12.59\,\mathrm{h}$ mean duration; Rodent: 20 recording sessions, $5.04\,\mathrm{h}$ mean duration). We analyzed high frequency activity (HFA, z-normalized analytical amplitude in the $70-150\,\mathrm{Hz}$ range; Fig. 1C/D, bottom) in both species to approximate coordinated population activity (Leonard et al., 2024; Leszczyński et al., 2020; Ray and Maunsell, 2011; Rich and Wallis, 2017; Watson et al., 2018; Manning et al., 2009). Specifically, we examined the HFA peak rate analogous to spike rate analyses, since HFA peaks are indicative of coordinated population firing. HFA power exhibits an approximate Gaussian distribution with a heavy tail distribution at z>1 (Fig. 1E/F, left); hence, we employed this threshold to define individual HFA peaks. A direct correlation between HFA and population firing had been established using the same dataset (Watson et al., 2018), supporting that HFA constitutes a proxy of coordinated population firing (Leonard et al., 2024; Parvizi and Kastner, 2018).

In humans (Fig. 1E, right), all prefrontal regions-of-interest (ROI) exhibited a higher peak rate than the MTL (Wilcoxon Rank Sum tests; all p < 0.001, FDR-corrected). The mPFC displayed the highest peak rate of the frontal ROIs (all p < 0.007), while OFC and dlPFC did not differ significantly (z = -1.14, p = 0.254, r = -0.074). Rodents displayed a highly comparable pattern (Fig. 1F, right) where the highest peak rate was observed in mPFC as compared to OFC and HC (all p < 0.042). However, peak rate was lower in the OFC than in HC (z = -3.43, p <0.001, r = -0.185). When directly comparing both species within the specified ROIs (Fig. 1G), we observed that humans exhibited a higher peak rate than rodents in the mPFC and OFC (all p < 0.001). Interestingly, the opposite pattern was evident in the HC, where peak rate in the rodent HC was higher than in the human MTL/HC (z = -10.57, p < -10.570.001, r = -0.637; for the full statistical report see Table S2). To investigate whether short, volatile HFA peaks bias these results towards higher peak frequencies, we additionally analyzed the widths of the detected peaks, but found no consistent relationships across regions, species and brain states (Figure S1).

Next, we estimated the information coding efficiency of the HFA signal using Shannon entropy. When assessing entropy and related information-theoretical metrics, differences in peak rate between regions and species pose a substantial challenge since entropy is constrained by (and increases with) the peak rate (i.e., the relative frequency, cf. Fig. 2B, bottom left; Pryluk et al., 2019; Rieke et al., 1999). As a direct result, information content is directly related to the HFA peak rate. To mitigate the dependency between peak rate and entropy and approximate the information content independent of the HFA peak rate, we employed a related information-theoretical metric, termed contrast entropy. Contrast entropy normalizes the observed information content of a signal relative to its own theoretical maximum, given a certain HFA peak rate (Pryluk et al., 2019). An intuitive description of contrast entropy is how many different neural patterns were observed, relative to the theoretical maximum. Hence, contrast entropy quantifies the amount of information a signal conveys, based on what it potentially could convey indicating the information coding efficiency of the neural population (Pryluk et al., 2019). In other words, contrast entropy quantifies the percentage of unique pattern combinations in the signal capturing pattern variability. Conversely, this metric is inversely correlated with pattern robustness (Pryluk et al., 2019). Here, we employ these terms interchangeably to contextualize the results.

To calculate *contrast entropy*, we first binarized the continuous, z-normalized HFA signal (Fig. 2A, top; *Methods*). Next, we defined a *neural pattern* (bin size). We employed various pattern lengths (4, 8 and 16; Fig. 2A, middle). For each pattern, we computed the population entropy and its analytical maximum (*Methods*; Fig. 2A, bottom). Lastly, we normalized the empirically observed entropy by the analytical maximum entropy to obtain the contrast entropy.

In order to validate the analytical approach, we first simulated ten one-hour trials of poisson-distributed peak trains from 1 to 30 Hz in integer steps (Fig. 2B, top). As expected, entropy is strongly related to peak rate (r(300) = 0.996, p < 0.001). This dependency is significantly



(caption on next page)

Fig. 1. Intracranial electrode placement, sleep recordings and high frequency activity peak statistics for humans and rodents. (A) Intracranial electrode placement in pharmaco-resistant epilepsy patients warped to MNI space with four regions-of-interest (top): dorsolateral prefrontal cortex (dIPFC; red), medial prefrontal cortex (mPFC; dark green), orbitofrontal cortex (OFC; light green) and medial temporal lobe (MTL; blue) including contacts in the Hippocampus (HC, bottom). (B) Schematic depiction of electrode placement in Long Evans rats using silicone probes with comparable coverage to the human sample in the mPFC, OFC and HC. (C) 1.5-hour excerpt from a full night's sleep of a single human subject with sleep stages (top) and corresponding HFA peak density (N per 30 s) of a mPFC (green) and a MTL (blue) electrode (bottom). (D) Same conventions as in C but for an exemplary sleep recording in a rat. (E) Left: probability density function (PDF) of the z-normalized HFA peak amplitudes across the whole night of all electrodes for each recording in humans. Peaks exceeded a HFA cutoff of 1 (blue) were considered as a proxy for multi-unit activity. Right: Peak rate for HFA peaks for each ROI. Depicted are PDFs and individual data points (median) for each electrode. Boxplots represent median, lower and upper quartiles and outlier-adjusted minimum and maximum values. Note, the higher peak rate in prefrontal ROIs as compared to the MTL. (F) Same conventions as in E but for rodents. (G) Same data as presented in E and F but visualized to compare both species. Note the overall higher peak rate in human prefrontal ROIs (circles) as compared to rodents (triangles), as well as the inversed pattern in rodent HC as compared to human MTL/HC.

reduced when accounting for peak rate using contrast entropy (Steiger test for dependent correlations: t(297)=38.18, p<0.001; r(300)=0.55, p<0.001). Note, that the residual correlations in simulated data reflects an additive effect that stems from the invariant peak rate across time at a given frequency. Thus, small correlations within one frequency are amplified when computing the correlation across the whole frequency range. Critically, this dependency was not present in empirical data (Fig. 2C). While we observed a high correlation between peak rate and entropy across all electrodes in humans and rodents (r(1599)=0.996, p<0.001; Fig. 2C, left), peak rate only explained 0.06 % of variance of contrast entropy ($r^2=0.006$, r(1599)=0.08, p<0.001; Steiger test vs. entropy correlation: t(1596)=62.105, p<0.001, Fig. 2C, right).

Moreover, entropy is not only impacted by peak rate but also by limited data sampling (Treves and Panzeri, 1995). To verify that the available data enabled appropriate sampling to estimate neural population efficiency, we analyzed contrast entropy in the simulated data across various time windows, pattern lengths and peak rates (Fig. 2D). These results demonstrate that longer neural patterns (larger bin size) require longer sampling intervals and higher peak rates to appropriately estimate contrast entropy. As expected, longer patterns displayed lower contrast entropy because of the coarser discretization, stronger dependency on data sampling and correlation of consecutive patterns (Pryluk et al., 2019). Importantly, all analyzed pattern lengths converged for recording durations of ~1 hour (Fig. 2E). Hence, the extensive data sampling during sleep recordings (up to 14 h) provides sufficient data to reliably estimate contrast entropy. Previously, various methods to estimate maximum entropy have been introduced and either determine maximum entropy based on the probability of a pattern given an empirical firing rate (Pryluk et al., 2019) or based on the probability of a peak occurring at a specific position within a pattern at a given empirical firing rate (Maoz et al., 2020). Here, we followed the definition of Maoz et al., but also implemented the alternative method. Both methods yielded nearly identical estimations of contrast entropy and were highly correlated (r = 0.973; p < 0.0001; mean correlation across all bin sizes).

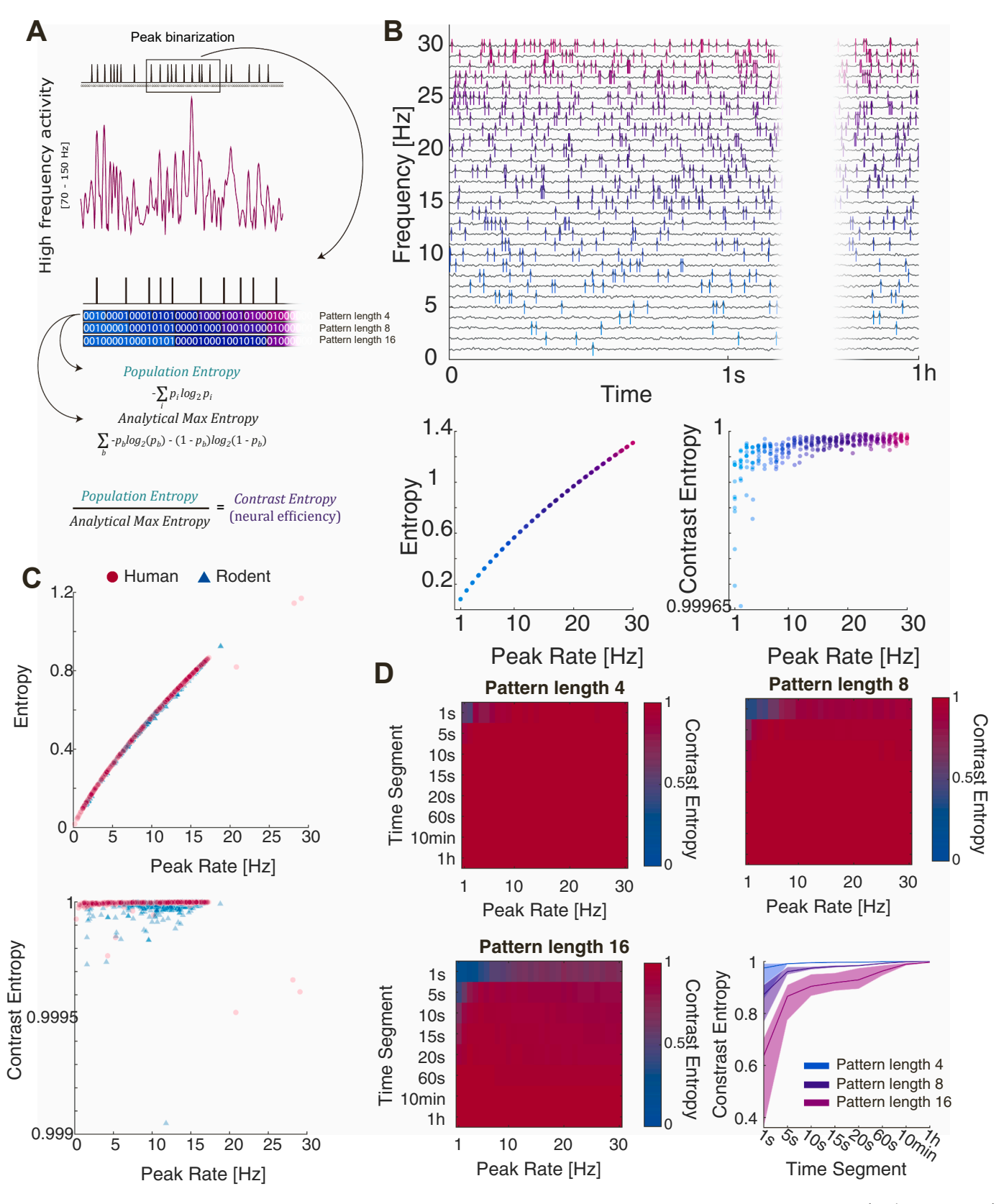
After having verified the analytical approach in simulations, we computed the contrast entropy of the continuous signal for humans and rodents within each ROI to determine which neural populations code information more efficiently (Fig. 3A). Our results demonstrated higher contrast entropy in human cortex as compared to their rodent homologues (Wilcoxon Rank Sum tests; all p < 0.001, FDR-corrected, Table S4). Note, that despite higher peak rates in rodent HC (Fig. 1G), we observed increased neural efficiency in the human MTL/HC (p <0.001). Humans also showed higher overall contrast entropy across all ROIs compared to rodents when the HFA amplitude constraint of z > 1was removed (Figure S2). Importantly, contrast entropy was higher in humans than in rodents regardless of neural pattern length (all p < 0.001; Fig. 3B). The differences between species increased as a function of neural pattern length (mean effect size $r_{pattern\ length\ 4} = 0.55$, $r_{pattern\ length}$ 8 = 0.70, $r_{pattern length 16} = 0.71$). Therefore, we report all results for a pattern length of 4 as the most conservative estimate to quantify differences between species. Moreover, we confirmed that differences between species were not driven by recording length differences. We predicted contrast entropy with the factors species and recording length using a robust linear regression. The overall model was significant ($R^2 = 0.684$, F(2,1596) = 1730, p < 0.001) and demonstrated that rodents exhibited lower contrast entropy than humans ($b = -1.86*10^{-6}$, p < 0.001) when accounting for recording length ($b = 3.36*10^{-7}$, p < 0.001)

To determine whether neural populations in evolutionary younger brain structures, such as the neocortex, exhibit higher information coding efficiency as compared to populations in evolutionary older structures (archicortex), we compared all ROIs within each species. In humans (Fig. 3C, top), we observed that contrast entropy in prefrontal areas was higher than in the MTL/HC (all p < 0.001), but did not differ significantly between the different prefrontal ROIs (all p > 0.239, also see Table S4). In rodents (Fig. 3C, bottom), the mPFC displayed higher contrast entropy than the OFC (z = 6.78, p < 0.001, r = 0.219) and the HC (z = 3.14, p = 0.002, r = 0.110). In sum, these results demonstrate that human neural populations exhibit higher information coding efficiency than rodents. In both species, we observed than neocortical regions were more efficient than archicortical areas.

To further dissect the contrast entropy differences between regions and species, we computed the observed probability of single and multiple HFA event patterns for 4-, 8- and 16-sized patterns (Figure S3). In line with the contrast entropy analyses, humans and the prefrontal cortex exhibited a higher probability to form multi-event patterns, i.e., more complex and less redundant patterns.

Next, we asked whether information coding efficiency differs between sleep stages. Given that there is no clear differentiation between NREM2 and NREM3 in rodents, we focused on wakefulness, NREM3 (just termed NREM from here on), and REM sleep. In order to resolve information coding per sleep stage, we computed entropy in 10 s segments and subsequently normalized it to its theoretical maximum across the entire recording. Note that the theoretical maximum is computed based on the average peak rate across different brain states. Thus, individual contrast entropy values may exceed a value of 1. This normalization approach restricted the subsequent analyses to within-species comparisons across different sleep stages.

Analyzing the sleep stage specific information coding dynamics within each ROI, we found that contrast entropy in the human dlPFC (Fig. 3D, top left) was lower during NREM-sleep than during wakefulness and REM-sleep (Wilcoxon Rank Sum tests; all p < 0.001, FDRcorrected, Table S5). Likewise, contrast entropy was lower during NREM-sleep as compared to wakefulness in the OFC and mPFC (all p <0.001). While contrast entropy was higher during wakefulness as compared to REM-sleep in the OFC (z = 4.76, p < 0.001, r = 0.43; Fig. 3D, top right), the opposite pattern was evident in the mPFC (z =-3.14, p < 0.001, r = -0.20; Fig. 3D, bottom left). In contrast, the human MTL/HC displayed no sleep stage specific changes in contrast entropy (all p > 0.22; Fig. 3D, bottom right). Importantly, we also verified that our analyses in human patients were not confounded by possible residual epileptic activity by detecting and removing segments with interictal epileptiform discharges (Figure S4). Furthermore, using within segment maximum entropy normalization confirmed these observations with decreasing contrast entropy from wakefulness to NREMsleep in all prefrontal ROIs (Figure S5). This pattern was absent in the



(caption on next page)

Fig. 2. Simulation of neural population information coding efficiency. (A) Schematic depiction of the analysis strategy. HFA as a proxy for multi-unit activity is discretized into peak trains. Peak trains are segmented according to a neural pattern length (i.e. elements per bin) of 4, 8 and 16. Population entropy is computed based on the probability (p_i) for each unique pattern. The peak rate of the same signal is used to calculate the analytical maximum entropy (p_b , i.e. probability of a peak at a given position in a given pattern). Normalizing the empirical population entropy by its theoretical maximum results in contrast entropy. Contrast entropy expresses the amount of information a signal conveys based on what it potentially could convey and therefore, indicates the efficiency of a signal. (B) Top: one hour of simulated poisson-distributed peak trains from 1 to 30 Hz in integer steps color coded by frequency. Bottom, left: relationship between peak rate und entropy for an exemplary pattern length of 4. Note the near perfect correlation. Bottom, right: relationship between peak rate and contrast entropy is strongly attenuated. (C) Empirical data from humans (red circles) and rodents (blue triangles) for all ROIs across the continuous recordings for an exemplary pattern length of 4. Left: strong relationship between peak rate and entropy as in panel B. Right: no correlation was observed between contrast entropy and peak rate. Note, neural populations of both species code information close the theoretical maximum. (D) Contrast entropy as a function of time segment length and peak rate for all three pattern lengths. In order to maximize contrast entropy, longer word length require higher peak rates and longer sampling intervals (E) Contrast entropy as a function of time collapsed over all frequencies for each pattern length (same data as in C). Note, with sufficient data sampling, contrast entropy irrespective of word length converges. Lines indicate the median, with shaded areas representing outlier ad

MTL.

In the rodent OFC and mPFC (Fig. 3E, top right & bottom left) contrast entropy decreased from wakefulness to NREM sleep (Wilcoxon Rank Sum tests; all p < 0.001, FDR-corrected, Table S6) but increased again from NREM to REM-sleep (all p < 0.001). Furthermore, during wakefulness both ROIs displayed higher contrast entropy than during REM-sleep (all p < 0.001). This was also the case when using within segment maximum entropy normalization (Figure S6). In contrast, rodent HC (Fig. 3E, bottom right), as also observed in humans, did not exhibit a significant difference between wakefulness and NREM dynamic (z = -0.95, p = 0.344, r = -0.07) but instead displayed higher contrast entropy during REM-sleep compared to wakefulness and NREM-sleep (all p < 0.001). Taken together, we found a striking accordance between the two species, demonstrating that information coding efficiency decreases in frontal cortices, but remains stable in the MTL/HC from wakefulness to NREM-sleep.

Next, similar to the species and regions pattern probability analyses (Figure S3), we also investigated the probability of forming multi-event neural patterns across sleep stages. Multi-event patterns were more likely to occur during wakefulness and REM-sleep compared to NREM-sleep in both species (Figure S7). Combined with the contrast entropy analyses these results suggest a more repetitive and, thus, less efficient neural code during NREM-sleep.

To assess whether sleep actively decreases information coding efficiency, we directly compared contrast entropy during wakefulness in the first half of the sleep recordings with the second half of the recordings in both species. As hypothesized, we observed a reduction information coding efficiency in humans for all recorded ROIs (Fig. 3F; Wilcoxon Rank Sum tests; all p < 0.030, FDR-corrected, Table S7). This was also the case when only comparing wakefulness periods before and after sleep (Figure S8). In contrast to humans, rodents' information coding efficiency increased in the OFC and mPFC from the first to the second half of the sleep recording (Fig. 3G; Wilcoxon Rank Sum tests; all p < 0.001, FDR-corrected, Table S8), which is likely due to a more fragmented sleep cycle. We found no differences for the rodent HC (p = 0.399). Note, isolating wakefulness periods before and after sleep was not possible in rodents due to limited data availability. In sum, these results demonstrate that information coding efficiency differs between species, regions and brain states.

Next, we addressed the relevance of the observed neural pattern variability for different behavioral states. We compared neural efficiency during cognitive engagement in the awake state (task and sleep recordings were available for subset of N=8 participants) as well as during medically-induced unconsciousness during electrode explantation (subset of N=6 participants) to coding efficiency during sleep and quiet wakefulness.

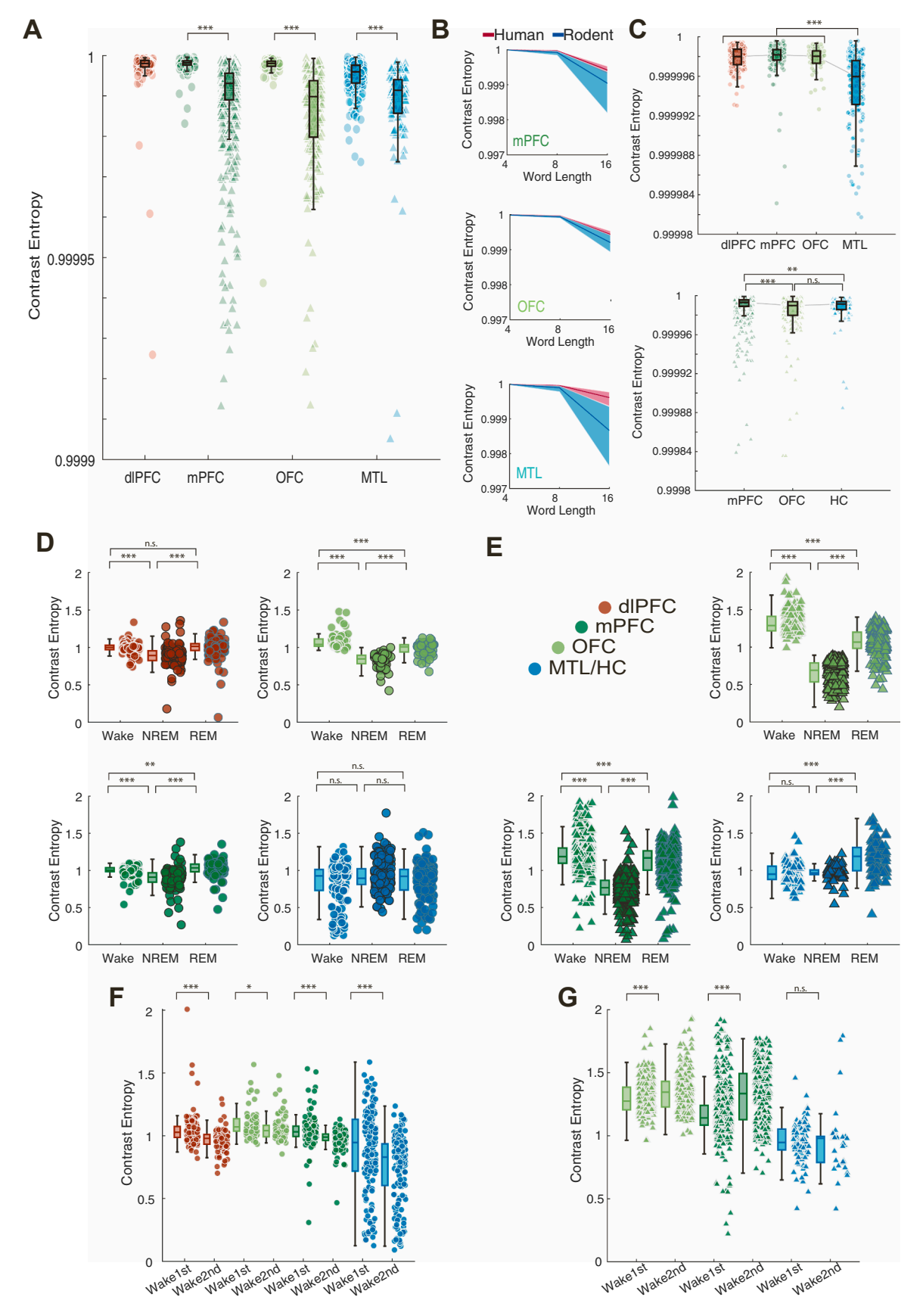
The visual search task required participants to memorize a given target orientation and maintain the representation throughout a delay phase (Fig. 4A). Subsequently, participants had to indicate on which side of the screen the target appeared. In the search condition, the three distractors were presented in the same color as the target. In the pop-out condition, distractors were displayed in a different color. We reasoned

that information coding efficiency should increase when the brain is actively processing information during task engagement. We calculated the contrast entropy in 6 s segments during task engagement irrespective of condition and in 6 s segments in the sleep recordings that were scored as wakefulness to match the trial duration and avoid a sampling bias. To counterbalance the trial counts between task and quiet wakefulness, data was randomly resampled and contrast entropy was calculated of a subset of the wakefulness data (1000 iterations). The subset was determined by the available trials of the task data for each patient. As hypothesized, contrast entropy increased during task engagement as compared to quiet wakefulness across all ROIs (Fig. 4B; Wilcoxon Rank Sum tests; all p < 0.001, FDR-corrected, Table S9). Note, contrast entropy values in the task data are lower compared to the sleep analyses because of shorter data segments (cf. Figure 2DE & 3A-C). Furthermore, we used 6 s second segments that included an overlap between trials in order to maximize segment length for a more accurate estimation. Importantly, analyzing shorter segments without overlap yielded similar results (Figure S9). This set of findings indicates that contrast entropy captures behaviorally relevant information coding efficiency.

Finally, we asked whether information coding efficiency decreases in states of altered arousal that do not promote memory consolidation like sleep. We analyzed contrast entropy while participants underwent propofol-induced general anesthesia. Concordant with the sleep stage analyses, we calculated contrast entropy by assessing entropy in 10 s segments and subsequently normalized it based on the maximum of the continuous signal. Propofol injection resulted in a steep decline in contrast entropy, with the decline marking the transition from wakefulness to unconsciousness (Fig. 4C). The decline in contrast entropy was a global effect, observed in all analyzed ROIs (Fig. 4D; Wilcoxon Rank Sum tests; all p < 0.001, FDR-corrected, Table S10). Furthermore, when comparing anesthesia to physiologic sleep, contrast entropy was lower as compared to NREM and REM sleep (all p < 0.001). To ensure, that our results are not due to non-stationaries caused by the propofol injection, we also compared contrast entropy before and after injection using within-segment maximum entropy normalization and withinsegment z-normalization. We observed consistent results, with an overall decrease in contrast entropy following injection (Figure S10). These results demonstrate that medically-induced unconsciousness disrupts information coding efficiency.

3. DISCUSSION

How does the sleeping brain store behaviorally relevant information, while discarding irrelevant information to free cognitive resources for the next day? Prominent theories of sleep function emphasize its importance for memory consolidation (Brodt et al., 2023; Klinzing et al., 2019), but sleep also improves other cognitive functions, including attention, problem-solving, cognitive flexibility and emotional regulation (Krause et al., 2017). It is well established that sleep facilitates learning and skill acquisition, but the neurophysiological mechanisms that explain why it is easier to imprint new information onto existing



(caption on next page)

Fig. 3. Species-, ROI-, and sleep stage-specific neural efficiency. (A) Contrast entropy for humans (circles) and rodent (triangles) for each ROI (pattern length 4). Individual data points represent the median per electrode. Boxplots depict the population median, lower and upper quartiles and outlier-adjusted minimum and maximum values (truncated for data visualization). Overall humans displayed higher contrast entropy for all ROIs. (B) Summary statistics for species contrasts per each ROI for every neural pattern length. Humans (red) have higher contrast entropy than rodents (blue) regardless of pattern length. Lines show the median, shaded areas represent outlier adjusted maxima and minima. (C) Top: ROI contrast for humans. Same conventions as in panel A. Prefrontal cortices display higher contrast entropy than the MTL/HC. Bottom: ROI contrast for rodents. Rodent mPFC exhibits higher contrast entropy than OFC and HC, but rodent HC displays higher contrast entropy than the rodent OFC. (D) Sleep stage resolved contrast entropy (entropy of 10 s segments normalized by the maximum entropy of the continuous recording) during wakefulness, NREM and REM of the human sample for dlPFC (red), mPFC (dark green), OFC (light green) and MTL (blue). All prefrontal ROIs display a similar dynamic with decreasing contrast entropy from wakefulness to NREM sleep and increasing contrast entropy from NREM to REM sleep. This pattern was absent in the MTL. Individual data points represent the median of an electrode across all trials per sleep stage. Boxplots depict the population median, lower and upper quartiles and outlier-adjusted minimum and maximum values. (E) Same conventions as in D but for rodents. Comparable sleep stage dynamics for rodents as compared to humans. Frontal cortices similarly decrease in contrast entropy from wakefulness between the first half of the sleep recoding and the second half in humans. All ROIs show a reduction in contrast entropy. (G) Same conventions as in F but for rodents. Prefrontal ROIs increase

circuits after sleep remain unknown. At the cellular level, it has been suggested that daytime learning is associated with synaptic potentiation, while sleep may re-regulate synaptic weights in a process that also been termed synaptic downscaling or pruning (Tononi and Cirelli, 2014). Hence, downscaling might reestablish the optimal milieu for next day learning. That a similar process occurs at the systems level so far remains largely speculative (Lendner et al., 2023).

Here, we employed an information-theoretical approach to estimate the information coding efficiency of neurophysiological population signals. In a comparative cross-species approach in rodents and humans, we demonstrate that (1) sleep reduces neural pattern variability, possibly reflecting the recapitulation of mnemonic information. (2) This reduction was most pronounced during NREM sleep in both species, (3) only occurred in the neocortex and (4) persisted after a full night of sleep. These observations could suggest that sleep-dependent memory consolidation might entail pattern repetition to form permanent engrams and highlights the importance of the neocortex as a presumed anatomical structure for long-term storage. While we did not conduct a sleep-dependent memory task to formally test this hypothesis, the behavioral relevance of the identified patterns was evident for increased pattern variability during cognitive engagement. In contrast, pattern variability was strongly attenuated during medically-induced loss of consciousness.

3.1. What constitutes information during sleep?

While previous research conceptualized sleep as a 'offline' state, recent work highlights its importance for active reprocessing of newly acquired information. Converging evidence across multiple lines of inquiry demonstrated that the sleeping brain actively recapitulates mnemonic information to selectively strengthen their representations, in a process termed replay (Wilson and McNaughton, 1994). Replay has mainly been observed at the cellular level in single neuron recordings in the rodent (Girardeau and Lopes-dos-Santos, 2021; Foster, 2017; Ólafsdóttir et al., 2018; Diba and Buzsaki, 2007) and human brain (Vaz et al., 2020, 2023), but may also take place at the systems level, amenable to LFP and EEG recordings (Brodt et al., 2023; Schreiner and Staudigl, 2020). Moreover, replay is temporally coupled to the periodic reoccurrence of large-scale neural oscillations during NREM sleep, specifically hippocampal sharp-wave ripples (SWR; ~100-200 Hz), which are in turn nested in thalamocortical spindles (~12-16 Hz) and cortical slow oscillations (Girardeau and Lopes-dos-Santos, 2021; Helfrich et al., 2019; Diekelmann and Born, 2010; Maingret et al., 2016; Rothschild et al., 2017; Staresina et al., 2015; Wilber et al., 2017). Hence, it is conceivable that neural pattern repetition, which is facilitated by sleep oscillations providing an endogenous timing mechanisms, might constitute a substrate of memory consolidation (Helfrich et al., 2021). This consideration raises the question how mnemonic information can be conceptualized and quantified in humans, not only at the cellular level, but also at the large-scale systems level.

Common approaches define information either as percent explain

variance (or correlation) of memory retention to SO, spindle or SWR activity (Gais et al., 2002; Hahn et al., 2020; Helfrich et al., 2018; Khodagholy et al., 2017; Schabus et al., 2004). Alternatively, information can be defined as decoding accuracy using multivariate pattern classifiers during endogenous and targeted memory reactivation (Cairney et al., 2018; Schonauer et al., 2017; Schreiner et al., 2021) or via the Shannon information theory framework (Luppi et al., 2024; Quian Quiroga and Panzeri, 2009; Helfrich et al., 2019). Information-theoretical metrics such as entropy, mutual information or Lempel-Ziv complexity have previously been shown to delineate different stages and quantify information flow during sleep (Abásolo et al., 2015; González et al., 2023; Helfrich et al., 2019; Höhn et al., 2024; Hou et al., 2021; Pascovich et al., 2022). A common finding is that information coding decreases during NREM sleep. However, the critical shortcoming of information theory is the strong dependence of entropy on the instantaneous neural activity. Neural firing rates are strongly attenuated during NREM sleep (Cirelli, 2017; Steriade et al., 2001) and hence, it is difficult to assess whether previous findings reflected limited information coding or whether they are the consequence of attenuated firing during NREM sleep. Here, we employed an analytical approach that quantifies the information content of a signal, which is normalized to its own theoretical maximum at a given activity rate (Pryluk et al., 2019). This approach enables the quantification of intrinsically generated neural activity patterns, irrespective of any outside variables, such as behavior or targeted memory reactivation.

Using this approach, we observed that the information coding efficiency is increased in neocortex as compared to archicortex. Moreover, it is also higher in humans than in rodents, and further increases during task engagement. Both observations suggest that diversified neural patterns could reflect a correlate of evolutionary younger and more developed brain structures, possibly underlying superior human cognitive abilities, which specifically rely on prefrontal cortex functionality (Pryluk et al., 2019; Carlén, 2017; Hanganu-Opatz et al., 2023; Laubach et al., 2018; Mendoza-Halliday et al., 2024; van Schalkwijk et al., 2023). In line with these findings, it has been argued that increased pattern variability makes the neural code more efficient, at the expense of pattern redundancy (Pryluk et al., 2019). A redundant coding scheme renders the neural code more reliable and robust, while a variable coding scheme might benefit cognitive flexibility. Our results replicate and extend the finding by Pryluk et al. (2019), who demonstrated a similar tradeoff between coding efficiency and robustness between subcortical and cortical regions in humans and non-human primates at the level of single neurons. Critically, these authors also observed the highest pattern variability in human neocortex. Conceptually, the increased variability has been suggested to support a synergistic coding scheme that formed during evolution to complement the evolutionary preserved archicortical system that is optimized for robustness. Hence, this is in accordance with the idea that sleep oscillations, which reflect recurrent and therefore, redundant neural patterns, are highly preserved across species.

A testable hypothesis for future studies is that a decrease in pattern

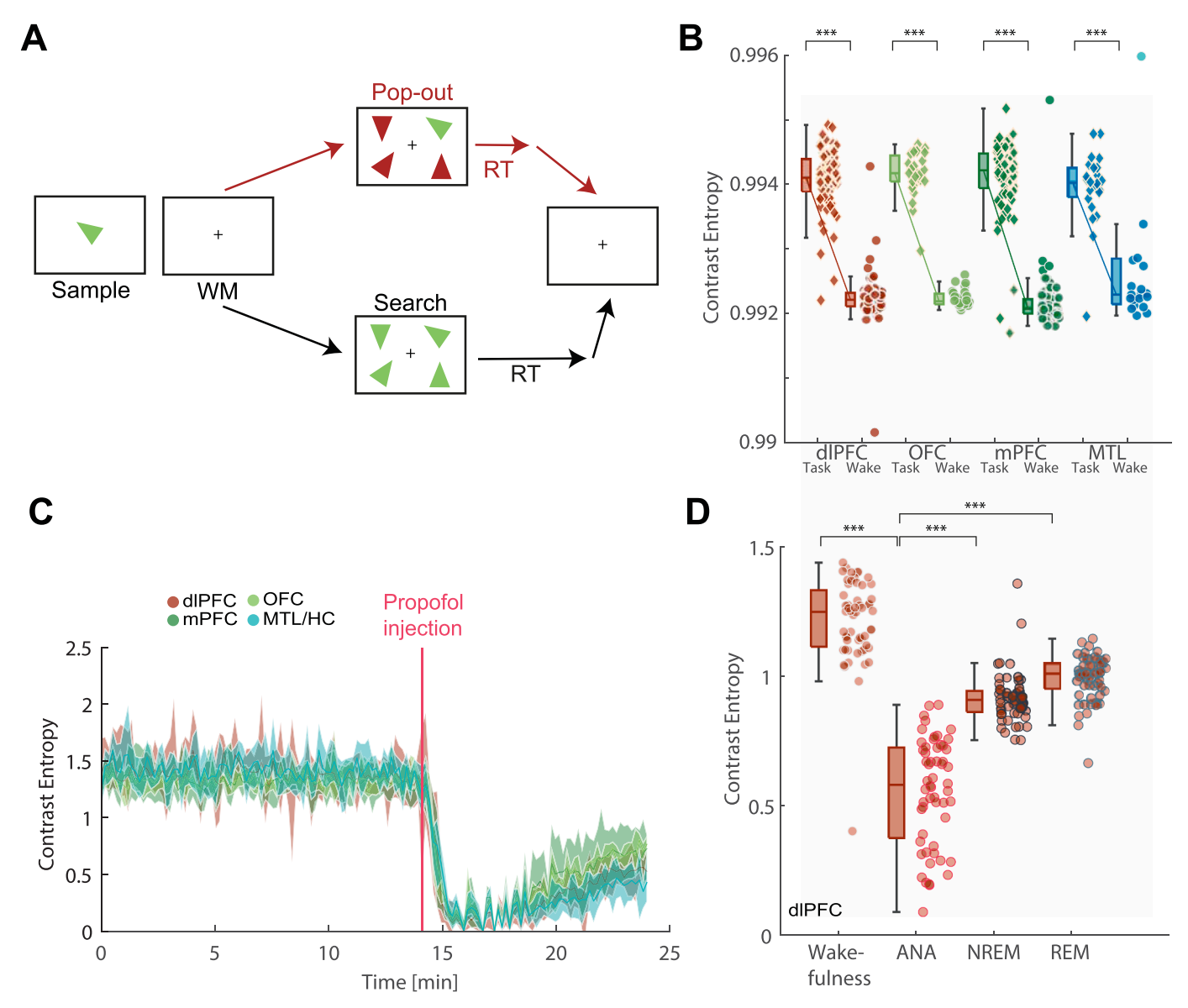


Fig. 4. Contrast entropy during cognitive engagement and medically-induced unconsciousness. (A) Visual search task (Slama et al. 2021). Target triangles (sample) with different colors and angles were presented for 1000 ms. After a short working memory delay (WM, 500 ms), participants indicated whether targets appeared on the left or right side. In the pop-out condition, the distractors differed in color from the target. In der search condition, distractors and target had the same color (RT, reaction time). (B) Contrast entropy for 6 s segments and a pattern length of 4 during task engagement (diamonds) and quiet wakefulness (circles) for all ROIs. Higher contrast entropy was evident during task engagement than during quiet wakefulness. Individual data points represent the median per electrode. Boxplots depict the population median, lower and upper quartiles and outlier-adjusted minimum and maximum values (C) Single subject example depicting the time course of contrast entropy (10 s segments normalized by the maximum entropy of the continuous recordings) before and after propofol injection during electrode explantation. Contrast entropy remains high during wakefulness, but rapidly declines upon propofol injection and remains low during medically-induced unconsciousness in all ROIs (dlPFC, red; mPFC, dark green; OFC, light green; MTL, blue). Lines show the median, shaded areas represent outlier adjusted maxima and minima. (D) Contrast entropy in 10 s segments normalized by the maximum entropy of the continuous recordings during wakefulness, anesthesia (ANA), NREM and REM sleep for dlPFC contacts (exemplary for all other ROIs) of a subset of patients. Same conventions as in B. The lowest contrast entropy was observed during anesthesia.

variability throughout the night correlates with memory consolidation. At the neurophysiological level, it is conceivable that the consolidation process and the associated reduction in pattern variability improves the signal-to-noise ratio. Hence, one prediction arising from these considerations is that decodability (pattern separability) is better once pattern variability has been decreased, which could indicate systems-level process of consolidation. In sum, the present results indicate that information-theoretical approaches could provide a complementary perspective to assess the memory function of the sleeping brain, by focusing on intrinsically generated neural patterns as the functional substrate of mnemonic information.

3.2. A hierarchy of information processing in the (sleeping) brain?

The MTL and PFC constitute two key nodes of the memory network. Converging evidence across multiple lines of inquiry gave rise to a conceptual model positing that newly acquired information is initially hippocampus-dependent by engaging hippocampal-neocortical loops (Rasch and Born, 2013; Frankland and Bontempi, 2005). Over the course of the consolidation process, mnemonic information is then permanently stored in the neocortex; hence, long-term memories progressively become independent of the hippocampus. At the cellular level, the neurophysiological substrate of long-term neocortical storage is likely a

modulation of synaptic weights enhancing neuroplasticity. It remains unclear if similar principles apply at the systems level amendable to LFP or EEG recordings. Here, we directly quantified the information coding efficiency of hippocampal and neocortical recordings. Our results are line with a model of overnight consolidation, where neocortical information content is high before sleep onset and lower after a full night of sleep. Importantly, a reduction in information coding efficiency during sleep is likely the result of pattern repetition, especially during NREM sleep, which may constitute a neurophysiological substrate of how new information is permanently imprinted onto existing neocortical circuits in a Hebbian manner (Buzsáki, 1998). In line with the systems consolidation model, we did not observe a strong overnight or sleep stage-dependent modulation in the hippocampus, possibly reflecting that the MTL does not constitute the structural correlate of long-term mnemonic storage. We also did not observe a strong modulation in rodents, which was likely the result of the fragmented sleep cycles that were characterized by frequent arousals. Our results are further supported by a recent human intracranial EEG study that demonstrated that non-oscillatory EEG background activity, which also captures neural variability, undergoes a downregulation of the course of a full night of sleep (Lendner et al., 2023). In sum, our results support the view that the neocortex may reflect an anatomical substrate of long-term storage. Moreover, the results demonstrate that information coding is more efficient in phylogenetically younger brain regions, especially in the human prefrontal cortex, which constitutes the key structure that enables unique human cognitive abilities.

3.3. Limitations and implications

In order to infer the information coding efficiency during sleep in a cross-species comparative design, we first employed simulations to determine the feasibility of the approach. Then, we performed the same analyses during rodent and human sleep. While we carefully controlled for a number of confounds and limitations, which arise from studying two different species using related methodologies, a number of important limitations and caveats remains.

First, brain anatomy and connectivity are vastly different between rodents and humans, especially the prefrontal cortex and its subdivisions (Carlén, 2017; Hanganu-Opatz et al., 2023; Laubach et al., 2018). Here, we recorded from putatively homologue regions, which are much larger in humans than in rodents and therefore, might differ in their dynamics. Second, while human NREM sleep is typically subdivided into three sub-stages, there is currently no clear consensus if rodent sleep exhibits the same number of sub-stages (Rayan et al., 2024). Hence, we focused on the presence of slow wave sleep, which dominates non-REM sleep in both species. Third, rodents exhibit more fragmented sleep cycles with frequent arousals as compared to humans. However, it needs to be highlighted that all human sleep recordings were carried out as part of clinical monitoring, which might have altered sleep properties due to specific circumstances in the clinical setting as exemplified by wakefulness, which was defined as spontaneous, unconstrained wakefulness before or after sleep and differs from the wakefulness experienced during states of high alertness or task engagement (cf. Fig. 4B). Fourth, differences between species also might be attributed the current pharmacological state of the patients. While the precise medication state could not be retrieved for the current participants, typical medications rather increase than decrease signal regularity (Limotai et al., 2020; Höller et al., 2018; Salinsky et al., 1994); hence, implying that we might have underestimated the true effect magnitude. Fifth, we assessed HFA, a proxy of population activity, to bridge the gap in recording modalities between both species. HFA has previously been shown to constitute a surrogate marker for neural population activity in humans with macroelectrodes (Leonard et al., 2024; Leszczyński et al., 2020) and in rodents with microelectrodes (Watson et al., 2018). Albeit these reports highlight that HFA might be comparable irrespective of the precise recording setup, we cannot rule out potential influences from the

recording modality and its spatial specificity. Collectively, these considerations might account for differences in peak rates between species. However, we observed that contrast entropy did account for these inherent differences and enabled studying similarity and differences between both species.

In addition, it is essential to consider that we interpret the present findings mainly in light of a sleep-dependent memory consolidation framework, which entails concepts, such as memory replay and synaptic homeostasis (Brodt et al., 2023; Tononi and Cirelli, 2014). Since we did not include a dedicated learning task data in our experimental design, it remains elusive how the identified patterns relate to mnemonic information processing. A testable hypothesis for future studies that arises from our findings is that the degree of information coding efficiency predicts overnight memory retention in sleep-dependent memory tasks. Moreover, it remains to be determined whether the coding efficiency correlates with mnemonic information as defined by decodability during targeted memory reactivation and how it relates to replay as commonly observed in rodent studies at the level of single neurons (Foster, 2017; Ólafsdóttir et al., 2018).

Lastly, we need to draw attention to the fact that other sources might have contributed to the reduced neural pattern variability during NREM sleep. For example, the lack of external input and recovery from prior wakefulness could render population activity more regular, sparse and lower dimensional (Vyazovskiy and Delogu, 2014). Indeed, a recent study demonstrated that decreased entropy during NREM sleep is attributed slow oscillation down states, which impose a repetitive pattern on neural firing (González et al., 2023). These slow oscillations are absent during REM sleep, where we observed overall higher contrast entropy compared to NREM sleep and, in one instance, even higher than during wakefulness (Fig. 3D). Hence, it appears plausible that REM sleep exhibits a higher degree of contrast entropy than quiet wakefulness before bedtime, which is accordance with the notion that REM sleep constitutes 'paradoxical sleep', which has been linked to vivid dreams, memory reactivation, and emotional processing (Simor et al., 2020).

In sum, despite these inherent differences and limitations, it is critical to highlight that we generally observed a high degree of concordance in information coding dynamics during human and rodent sleep.

3.4. Conclusions

In this cross-species intracranial neurophysiology study, we demonstrate a tradeoff in the neural population code in rodents and humans during sleep. Our findings appear to align with a model where pattern repetition during sleep may play a role in the consolidation process, which seems to primarily involve the neocortex. These results suggest that neural pattern variability may be an indicator of information accumulation, which appears to undergo a process of renormalization during sleep. This could potentially facilitate the clearance of cognitive resources, allowing for more efficient processing the following day.

4. Materials and methods

REAGENT or RESOURCE	SOURCE	IDENTIFIER
Software and algorithm	ns	
EPrime	Psychology Software Tools	https://pstnet.com/
MATLAB 2021a	Mathworks	http://www.mathworks.com
FieldTrip 20210912	Oostenveld et al., 2011	https://www.fieldtriptoolbox.org/
Maximum Entropy toolbox	Maoz et al., 2017	https://orimaoz.github.io/maxent_toolbox/

4.1. RESOURCE AVAILABILITY

4.1.1. Lead contact

Further information and requests for resources and reagents should be directed to and will be fulfilled by the lead contact (michael.hahn@uni-tuebingen.de).

4.1.2. Materials availability

This study did not generate new unique reagents.

4.1.3. Data and code availability

Freely available software and algorithms used for analysis are listed in the resource table. All custom code in this manuscript is available upon request from the Lead Contact.

4.1.4. Subjects

4.1.4.1. Human participants. Data of 19 patients (age: 19 - 58 years; 9 female) with pharmacoresistent epilepsy were recorded during seizure onset zone diagnostics with implanted stereotactic depth electrodes (Ad-Tech, 5 mm electrode spacing) at the University of California Irvine Medical Center, USA. Electrode implantation scheme was solely based on clinical considerations but participants that entered analyses were selected according to relevant electrode placement in the dlPFC, mPFC, OFC and MTL. Before participating in the study, all patients provided written informed consent. The study was conducted in accordance with the Declaration of Helsinki and approved by the Institutional Review Board at the University of California, Irvine (number: 2014-1522) as well as by the Committee for Protection of Human Subjects at the University of California, Berkeley (number: 2010-02-783). Main analyses comparing species and ROIs were conducted with N = 16 participants with concurrent coverage in all ROIs (19 - 58 years; 8 female). When available, we also analyzed task data and anesthesia data during electrode explantation in two subsets of participants (task subsample: N = 8, age: 22 - 50 years, 5 females; anesthesia subsample: N = 6, age: 25 - 58years, 3 female). Note, three subjects without simultaneous ROI coverage, which are not included in the main analyses, were added to the anesthesia subsample due to the low sample size.

4.1.4.2. Rodents. Rodent data was acquired from an open dataset containing LFP data of 11 male Long-Evans rats (weight: 250 – 500 g, age: 3 – 7 months) with 27 recording sessions (Watson et al., 2016b). Based on our pre-specified ROIs, we analyzed 20 recording sessions of eight rodents with coverage in the mPFC, OFC and HC. Sleep data of the freely behaving animals was recorded in their home cage during daytime with no specific behavior paradigm. Recordings lasted between one and eight hours. One or two 64-site silicon probes (Buzsaki64 or Buzsaki64sp models from NeuroNexus, Ann Arbor, MI) were implanted 0.5 mm above frontal cortical regions and/or dorsal Hippocampus with < 300 µm advancements per day using a microdrive. For a more detailed description of the rodent dataset and procedures, please see Watson et al., (2016a, 2016b, & 2018).

4.1.5. Behavioral task

Participants completed a visual search task (Fig. 4A; for more details see Li et al., 2010; Slama et al., 2021). Stimuli were presented on a laptop at the participants bed side using E-Prime 2.0 software (Psychology Software Tools). In brief, a target triangle with a given color and tilted at a given angle (0°, 45°, 90°, 135°, 180°, 225°, 270°, or 315°) was presented for 1000 ms. After a short memory delay (500 ms), the target with three distractors appeared again. Two stimuli were presented on the left side of the screen and two on the right side. Then participants indicated whether the target appeared on the left or right side with a button press. In the pop-out condition, the distractors exhibited a distinct color compared to the target. In the search condition, both

distractors and the target shared the same color, with the sole distinction being the tilt angle. Participants had a response window of up to 2000 ms. The response was followed by a 1000 ms inter trial interval with a fixation cross. The task comprised four blocks, each containing 32 trials. Half of these trials were designated as search trials, while the remaining half were categorized as pop-out trials. Conditions were presented in randomized order. For analyses we segmented the data into $-2000\ \mathrm{ms} - 4000\ \mathrm{ms}$ epochs relative to target triangle onset.

4.1.6. iEEG data acquisition and preprocessing

4.1.6.1. Human. We collected electrophysiological data with a 256-channel Nihon Kohden recording device (JE120A). The signal was recorded at 5 kHz sampling rate and analog filtered at 0.01 Hz. For analyses, we selected contacts with dlPFC, mPFC and OFC placement. The MTL ROI comprised electrodes within and in close proximity to the hippocampus as well as in the entorhinal cortex (Helfrich et al., 2019). Electrode placement was verified in native space by two independent neurologists. Electrophysiological data were analyzed using Matlab 2021a (Mathworks Inc) and the Fieldtrip Toolbox (Oostenveld et al., 2011) as well as custom written code. To appreciate the electrode distribution across the whole sample, we subsequently warped electrode placement to MNI space for visualization purposes only (Fig. 1A). We demeaned the continuous data and down-sampled to 500 Hz. To approximate a local field potential, we bipolar referenced each contact to the closest neighbor along the depth electrode.

4.1.6.2. Interictal epileptiform discharge detection. To detect interictal epileptiform discharges (IED) we employed an established automatic detection algorithm (Gelinas et al., 2016). In brief, we filtered the continuous signal with a two-way least-squares FIR filter between 25 and 80 Hz. Next, we extracted the analytical amplitude via the Hilbert transform and subsequently z-scored the signal. An IED event was identified if the signal exceeded the mean by three standard deviations for at least 20 ms and no more than 100 ms.

4.1.6.3. Rodent. Data were recorded using a 256-channel Amplipex recording system (Szeged, Hungary) at 20 kHz sampling rate and after 400x headstage gain. The continuous data were low-pass-filtered to 1250 Hz in order to obtain the local field potential. Additionally, we demeaned the signal and re-referenced every channel against the average activity within the specified ROI. The signal was subsequently down-sampled to 500 Hz to match the sampling rate for the human recordings.

4.1.7. Sleep staging

4.1.7.1. Human. In addition to intracranial electrodes, we recorded scalp EEG to support sleep staging based on Rechtschaffen & Kales criteria (Rechtschaffen and Kales, 1968) using the same Nihon Kohden recording system. Coverage typically included Fz, Cz, C3, C4, and Oz placed according to the 10–20 system. For REM sleep classification, we placed four Electroculogram (EOG) using four electrodes placed around the right and left outer canthi. To obtain a surrogate electromyogram (EMG) signal, we high-pass filtered either the ECG or EEG channels that were close to neck or skeletal muscles above 40 Hz (Helfrich et al., 2019). Sleep stages were classified in 30 second epochs by an expert human scorer. We combined sleep stage S3 and S4 to NREM3 in order adhere to the international AASM standard (Iber et al., 2007).

4.1.7.2. Rodent. For the sleep analyses in rodents, we utilized the provided sleep stages from the original study (for more detail see Watson et al., 2016). In brief, a broadband LFP and a narrowband theta frequency band LFP ratio signal (5–10 Hz/2–16 Hz) were extracted from

Spectrograms using a sliding window FFT (10 s window, 1 s steps) at frequencies between 1 and 100 Hz (log-spaced) Next, principal components (PC) form the broadband LFP signal of a cortical probe were extracted. The first PC captured the variation of synchronized (i.e. NREM) and desynchronized states (Wakefulness & REM) based on low frequency power (< 20 Hz). The theta ratio was extracted from channels (preferably hippocampal contacts when available) with the most prominent theta signal upon manual inspection. The EMG signal was constructed from intracranial data by computing zero time-lag correlation coefficients between two signals filtered in the 300 - 600 Hz range from different channels with a minimum distance of at least two shanks. All pairwise correlations calculated in each 0.5 s bin were averaged to obtain an EMG score. NREM stage was identified with a high LFP PC1 and a low EMG, whereas REM stage was identified with a high Theta and low EMG. A third, diffuse state was marked by low broadband LFP, higher EMG and Theta. The sleep scoring algorithm involved multiple divisions, with thresholds established at the points where the troughs separated the peaks in the distributions of the PC1, Theta and EMG metrics. All automated scorings were manually verified and corrected if necessary.

4.1.8. Anesthesia

For human subjects only, we obtained intracranial anesthesia data during electrode explantation up to the point of electrode removal. Before the procedure, all patients resumed their usual antiepileptic medication regime and received up to 2 mg of midazolam as premedication. To induce anesthesia, patients were administered an intravenous injection of Propofol, with the dosage ranging from 50 mg to 200 mg, tailored to individual needs. Half of the patients also received between 50 mcg and 100 mcg of Fentanyl for pain management and to balance anesthesia. During the explantation procedure, Remifentanil, Propofol or Sevoflurane were injected for anesthetic maintenance. All procedures were conducted at the University of California Irvine Medical Center.

4.1.9. iEEG analysis

4.1.9.1. High frequency activity and peak detection. For both species we extracted the instantaneous amplitude of the filtered continuous signal via the Hilbert transform in the 70-150 Hz frequency range. Next, we znormalized the signal per channel in the time domain. Subsequently, we extracted the HFA peak amplitudes using the findpeaks.m matlab function (default settings; no additional peak distance or peak width criteria) and binarized the signal for every peak exceeding the threshold of z=1. While there is no consensus in literature about a definitive HFA frequency range, which is often defined from 50 Hz upwards, we opted for the frequently employed 70-150 Hz range to avoid line-noise at 60 Hz (Leonard et al., 2024; Leszczyński et al., 2020; Parvizi and Kastner, 2018; Rich and Wallis, 2017; Helfrich et al., 2019). Importantly, activity in this frequency range has been demonstrated to be directly correlated to multi-unit activity (Leonard et al., 2024; Leszczyński et al., 2020; Rich and Wallis, 2017).

4.1.9.2. Contrast entropy. We calculated contrast entropy to approximate the information content of the neural population firing independent of the HFA peak rate. Contrast entropy is an information theoretical measure that normalizes a signal's observable information content by its theoretical maximum, given an empirical firing rate and has been previously employed in a cross-species single-unit study (Pryluk et al., 2019). Here, to obtain the contrast entropy of a surrogate of multi-unit activity, we first binarized the continuous, z-normalized HFA signal (Fig. 2A, top; threshold at z = 1). To discount epileptic activity in the human sample, all peaks in the binarized HFA signal were adjusted to zero \pm 200 ms surrounding an IED peak. Next, we defined a neural pattern (segment length or bin size). We employed various pattern

lengths (4, 8 and 16; Fig. 2A, middle). For each pattern length, we computed the population entropy and its analytical maximum (Fig. 2A, bottom). Lastly, we normalized the empirically observed entropy by the analytical maximum entropy (Pryluk et al., 2019; Maoz et al., 2020) to obtain the contrast entropy. Hence, contrast entropy quantifies the amount of information a signal conveys, based on what it potentially could convey and therefore, indicates the efficiency of the neural population (Pryluk et al., 2019).

Population entropy was computed using the formula where p_i is the probability of a unique pattern given a specified pattern length:

$$Entropy = -\sum_{i} p_i \log_2 p_i$$

The analytical maximum entropy (Maoz et al., 2020; Maoz and Schneidman, 2017) is given by the equation:

$$\textit{MaxEntropy} = \sum_b -p_b log_2(p_b) - (1-p_b) log_2(1-p_b)$$

Where p_b is the probability of the occurrence of a HFA peak at a given position b in a given pattern based on the empirical peak rate. In the last step, we normalized the population entropy by the analytical maximum entropy to estimate contrast entropy:

$$Contrast \ Entropy = \frac{Entropy}{MaxEntropy}$$

We calculated contrast entropy in two ways. (1) computing entropy and maximum entropy on the continuous signal of the whole recording for the most precise estimate due to maximized data sampling (Fig. 3A/B/C). (2) Computing entropy in 10 second segments, which we subsequently normalized based on the maximum entropy of the continuous recording to resolve sleep stage specific coding dynamics (Fig. 3D/E & Fig. 4C/D). For humans, we also calculated contrast entropy in 6 second segments to compare task data to sleep data (Fig. 4A/B).

4.1.10. Simulation

We simulated one hour of Poisson-distributed peak trains with constant frequencies between 1 and 30 Hz for each integer step (Fig. 2B/D). For each frequency step, we stimulated 10 trials with a 500 Hz sampling rate to match the features of the empirical recordings. The probability of a peak appearing in a given time bin $\Delta t = \frac{1}{Sampling\ rate}$ is given by $fr * \Delta t$, where fr denotes the constant frequency. For each time bin, a peak appears if $x < fr * \Delta t$, where x is a random number drawn from a uniform distribution between 0 and 1 (Dayan and Abbott, 2001).

4.1.11. Statistical testing

We conducted Wilcoxon rank sum tests to assess the differences between species and ROIs unless stated otherwise (Fig. 1E/F/G, Fig. 3 & Fig. 4B/D). For effect sizes, we reported "r" as a standardized metric using the formula:

$$r = \frac{z}{\sqrt{N}}$$

Where z is the test statistic of the Wilcoxon rank sum test and N the sample size. To maintain the integrity of our findings, all p values were corrected using the false discovery rate (FDR) method (Benjamini and Hochberg, 1995). To address the potential impact of varying recording lengths between species (Fig. 3A), we utilized a robust linear regression model with a bi-square weight function and a default tuning constant of 4.685. We modeled the regression with the formula Contrast Entropy $\sim 1 + \text{Species} + \text{Recording length}$.

In addition, we performed Pearson correlational analyses to assess the relationships between peak rate and entropy/contrast entropy (Fig. 2B/C). To determine whether correlations between variables were significantly different, we computed Steiger Z tests (Steiger, 1980).

CRediT authorship contribution statement

Katarina S.J. Slama: Investigation. Matthias Anwander: Investigation. Janna D. Lendner: Writing – review & editing, Resources, Investigation. Michael A. Hahn: Writing – original draft, Visualization, Methodology, Investigation, Formal analysis, Conceptualization. Randolph F. Helfrich: Writing – original draft, Supervision, Resources, Methodology, Funding acquisition, Conceptualization. Jack J. Lin: Writing – review & editing, Resources, Investigation. Robert T. Knight: Writing – review & editing, Resources, Investigation.

Declaration of Competing Interest

The authors declare that they have no known competing financial interests or personal relationships that could have appeared to influence the work reported in this paper.

Data availability

Data will be made available on request.

Acknowledgements

This work was funded by the German Research Foundation, Emmy Noether Program (DFG HE8329/2–1; RFH), the Hertie Foundation, Network for Excellence in Clinical Neuroscience (RFH), the Jung Foundation for Research and Science (Ernst Jung Career Advancement Award in Medicine; RFH), the Medical Faculty of the University of Tübingen (JRG Plus program; RFH), the German National Academic Exchange Service (DAAD) with funds from the German Federal Ministry of Education and Research (PRIME program, MAH) and the National Institutes of Health (U19NS107609; RTK, JJL) as well as an NIMH Conte Center Grant (1 PO MH109429, RTK) and NINDS (2 R01 NS021135, RTK).

Appendix A. Supporting information

Supplementary data associated with this article can be found in the online version at doi:10.1016/j.pneurobio.2024.102672.

References

- Abásolo, D., Simons, S., Morgado da Silva, R., Tononi, G., Vyazovskiy, V.V., 2015. Lempel-Ziv complexity of cortical activity during sleep and waking in rats. J. Neurophysiol. 113, 2742–2752. https://doi.org/10.1152/jn.00575.2014.
- Benjamini, Y., Hochberg, Y., 1995. Controlling the False Discovery Rate: A Practical and Powerful Approach to Multiple Testing. J. R. Stat. Soc. Ser. B Methodol. 57, 289–300. https://doi.org/10.1111/j.2517-6161.1995.tb02031.x.
- Brodt, S., Inostroza, M., Niethard, N., Born, J., 2023. Sleep—A brain-state serving systems memory consolidation. Neuron 111, 1050–1075. https://doi.org/10.1016/j. neuron.2023.03.005.
- Buzsáki, G., 1998. Memory consolidation during sleep: a neurophysiological perspective. J. Sleep. Res. 7, 17–23. https://doi.org/10.1046/j.1365-2869.7.s1.3.x.
- Cairney, S.A., Guttesen, A.A.V., El Marj, N., Staresina, B.P., 2018. Memory Consolidation Is Linked to Spindle-Mediated Information Processing during Sleep. e4 Curr. Biol. 28, 948–954. https://doi.org/10.1016/j.cub.2018.01.087.
- Carlén, M., 2017. What constitutes the prefrontal cortex? Science 358, 478–482. https://doi.org/10.1126/science.aan8868.
- Cirelli, C., 2017. Sleep, synaptic homeostasis and neuronal firing rates. Curr. Opin. Neurobiol. 44, 72–79. https://doi.org/10.1016/j.conb.2017.03.016.
- Dayan, P., Abbott, L.F., 2001. Theoretical neuroscience: computational and mathematical modeling of neural systems. Massachusetts Institute of Technology Press.
- Diba, K., Buzsaki, G., 2007. Forward and reverse hippocampal place-cell sequences during ripples. Nat. Neurosci. 10, 1241–1242. https://doi.org/10.1038/nn1961.
- Diekelmann, S., Born, J., 2010. The memory function of sleep. Nat. Rev. Neurosci. 11, 114–126. https://doi.org/10.1038/nrn2762.
- Euston, D.R., Tatsuno, M., McNaughton, B.L., 2007. Fast-Forward Playback of Recent Memory Sequences in Prefrontal Cortex During Sleep. Science 318, 1147–1150. https://doi.org/10.1126/science.1148979.
- Foster, D.J., 2017. Replay Comes of Age. Annu. Rev. Neurosci. 40, 581–602. https://doi.org/10.1146/annurev-neuro-072116-031538.

- Frankland, P.W., Bontempi, B., 2005. The organization of recent and remote memories. Nat. Rev. Neurosci. 6, 119–130. https://doi.org/10.1038/nrn1607.
- Gais, S., Molle, M., Helms, K., Born, J., 2002. Learning-dependent increases in sleep spindle density. J. Neurosci. 22, 6830–6834.. https://doi.org/10.1523/ JNEUROSCI.22-15-06830.2002.
- Gelinas, J.N., Khodagholy, D., Thesen, T., Devinsky, O., Buzsáki, G., 2016. Interictal epileptiform discharges induce hippocampal-cortical coupling in temporal lobe epilepsy. Nat. Med. 22, 641–648. https://doi.org/10.1038/nm.4084.
- Girardeau, G., Lopes-dos-Santos, V., 2021. Brain neural patterns and the memory function of sleep. Science 374, 560–564. https://doi.org/10.1126/science.abi8370.
- González, J., Cavelli, M., Tort, A.B.L., Torterolo, P., Rubido, N., 2023. Sleep disrupts complex spiking dynamics in the neocortex and hippocampus. PLOS ONE *18*, e0290146. https://doi.org/10.1371/journal.pone.0290146.
- Hahn, M.A., Heib, D., Schabus, M., Hoedlmoser, K., Helfrich, R.F., 2020. Slow oscillation-spindle coupling predicts enhanced memory formation from childhood to adolescence. Elife 9. https://doi.org/10.7554/eLife.53730.
- Hanganu-Opatz, I.L., Klausberger, T., Sigurdsson, T., Nieder, A., Jacob, S.N., Bartos, M., Sauer, J.-F., Durstewitz, D., Leibold, C., Diester, I., 2023. Resolving the prefrontal mechanisms of adaptive cognitive behaviors: A cross-species perspective. Neuron 111, 1020–1036. https://doi.org/10.1016/j.neuron.2023.03.017.
- Helfrich, R.F., Lendner, J.D., Knight, R.T., 2021. Aperiodic sleep networks promote memory consolidation. Trends Cogn. Sci. 25, 648–659. https://doi.org/10.1016/j. tics.2021.04.009.
- Helfrich, R.F., Lendner, J.D., Mander, B.A., Guillen, H., Paff, M., Mnatsakanyan, L., Vadera, S., Walker, M.P., Lin, J.J., Knight, R.T., 2019. Bidirectional prefrontalhippocampal dynamics organize information transfer during sleep in humans. Nat. Commun. 10, 3572. https://doi.org/10.1038/s41467-019-11444-x.
- Helfrich, R.F., Mander, B.A., Jagust, W.J., Knight, R.T., Walker, M.P., 2018. Old brains come uncoupled in sleep: slow wave-spindle synchrony, brain atrophy, and forgetting. e4 Neuron 97, 221–230. https://doi.org/10.1016/j.neuron.2017.11.020.
- Höhn, C., Hahn, M.A., Lendner, J.D., Hoedlmoser, K., 2024. Spectral Slope and Lempel–Ziv Complexity as Robust Markers of Brain States during Sleep and Wakefulness. eNeuro 11. https://doi.org/10.1523/ENEURO.0259-23.2024.
- Höller, Y., Helmstaedter, C., Lehnertz, K., 2018. Quantitative pharmacoelectroencephalography in antiepileptic drug research. CNS Drugs 32, 839–848. https://doi.org/10.1007/s40263-018-0557-x.
- Hou, F., Zhang, L., Qin, B., Gaggioni, G., Liu, X., Vandewalle, G., 2021. Changes in EEG permutation entropy in the evening and in the transition from wake to sleep. Sleep 44. zsaa226. https://doi.org/10.1093/sleep/zsaa226.
- Iber, C., Ancoli-Israel, S., Chesson, A., Quan, S.F., 2007. The AASM Manual for the Scoring of Sleep and Associated Events: Rules, Terminology, and Technical Specification, Second ed. American Academy of Sleep Medicine.
- Jiang, X., Shamie, I., K. Doyle, W., Friedman, D., Dugan, P., Devinsky, O., Eskandar, E., Cash, S.S., Thesen, T., Halgren, E., 2017. Replay of large-scale spatio-temporal patterns from waking during subsequent NREM sleep in human cortex. Sci. Rep. 7, 17380. https://doi.org/10.1038/s41598-017-17469-w.
- Khodagholy, D., Gelinas, J.N., Buzsáki, G., 2017. Learning-enhanced coupling between ripple oscillations in association cortices and hippocampus. Science 358, 369–372. https://doi.org/10.1126/science.aan6203.
- Klinzing, J.G., Niethard, N., Born, J., 2019. Mechanisms of systems memory consolidation during sleep. Nat. Neurosci. 22, 1598–1610. https://doi.org/10.1038/ s41593-019-0467-3.
- Krause, A.J., Simon, E.B., Mander, B.A., Greer, S.M., Saletin, J.M., Goldstein-Piekarski, A. N., Walker, M.P., 2017. The sleep-deprived human brain. Nat. Rev. Neurosci. 18, 404–418. https://doi.org/10.1038/nrn.2017.55.
- Laubach, M., Amarante, L.M., Swanson, K., White, S.R., 2018. What, if anything, is rodent prefrontal cortex? eneuro 5, ENEURO.0315-18.2018. https://doi.org/ 10.1523/ENEURO.0315-18.2018
- Lendner, J.D., Niethard, N., Mander, B.A., van Schalkwijk, F.J., Schuh-Hofer, S., Schmidt, H., Knight, R.T., Born, J., Walker, M.P., Lin, J.J., et al., 2023. Human REM sleep recalibrates neural activity in support of memory formation. Sci. Adv. 9, eadj1895. https://doi.org/10.1126/sciadv.adj1895.
- Leonard, M.K., Gwilliams, L., Sellers, K.K., Chung, J.E., Xu, D., Mischler, G., Mesgarani, N., Welkenhuysen, M., Dutta, B., Chang, E.F., 2024. Large-scale single-neuron speech sound encoding across the depth of human cortex. Nature 626, 593–602. https://doi.org/10.1038/s41586-023-06839-2.
- Leszczyński, M., Barczak, A., Kajikawa, Y., Ulbert, I., Falchier, A.Y., Tal, I., Haegens, S., Melloni, L., Knight, R.T., Schroeder, C.E., 2020. Dissociation of broadband high-frequency activity and neuronal firing in the neocortex. Sci. Adv. 6, eabb0977. https://doi.org/10.1126/sciadv.abb0977.
- Li, L., Gratton, C., Yao, D., Knight, R.T., 2010. Role of frontal and parietal cortices in the control of bottom-up and top-down attention in humans. Brain Res 1344, 173–184. https://doi.org/10.1016/j.brainres.2010.05.016.
- Limotai, C., Phayaph, N., Pattanasilp, B., Mokklaew, J., Limotai, N., 2020. Effects of antiepileptic drugs on electroencephalography (EEG): insights and applicability. Epilepsy Behav. 110, 107161. https://doi.org/10.1016/j.yebeh.2020.107161.
- Liu, Y., Dolan, R.J., Kurth-Nelson, Z., Behrens, T.E.J., 2019. Human replay spontaneously reorganizes experience. Cell 178, 640–652.e14. https://doi.org/10.1016/j. cell.2019.06.012.
- Luppi, A.I., Rosas, F.E., Mediano, P.A.M., Menon, D.K., Stamatakis, E.A., 2024. Information decomposition and the informational architecture of the brain. Trends Cogn. Sci. 0. https://doi.org/10.1016/j.tics.2023.11.005.
- Maingret, N., Girardeau, G., Todorova, R., Goutierre, M., Zugaro, M., 2016. Hippocampocortical coupling mediates memory consolidation during sleep. Nat. Neurosci. 19, 959–964. https://doi.org/10.1038/nn.4304.

- Manning, J.R., Jacobs, J., Fried, I., Kahana, M.J., 2009. Broadband shifts in local field potential power spectra are correlated with single-neuron spiking in humans. J. Neurosci. 29, 13613–13620. https://doi.org/10.1523/JNEUROSCI.2041-09.2009.
- Maoz, O., Schneidman, E., 2017. maxent toolbox: maximum entropy toolbox for MATLAB. Version Version 1 (02).
- Maoz, O., Tkačik, G., Esteki, M.S., Kiani, R., Schneidman, E., 2020. Learning probabilistic neural representations with randomly connected circuits. Proc. Natl. Acad. Sci. 117, 25066–25073. https://doi.org/10.1073/pnas.1912804117.
- Mendoza-Halliday, D., Major, A.J., Lee, N., Lichtenfeld, M.J., Carlson, B., Mitchell, B., Meng, P.D., Xiong, Y., Sophy, Westerberg, J.A., Jia, X., et al., 2024. A ubiquitous spectrolaminar motif of local field potential power across the primate cortex. Nat. Neurosci. 27, 547–560. https://doi.org/10.1038/s41593-023-01554-7.
- Ólafsdóttir, H.F., Bush, D., Barry, C., 2018. The role of hippocampal replay in memory and planning. Curr. Biol. 28, R37–R50. https://doi.org/10.1016/j.cub.2017.10.073.
- Oostenveld, R., Fries, P., Maris, E., Schoffelen, J.-M., 2011. FieldTrip: open source software for advanced analysis of MEG, EEG, and invasive electrophysiological data. Comput. Intell. Neurosci. 2011, 156869. https://doi.org/10.1155/2011/156869.
- Parvizi, J., Kastner, S., 2018. Promises and limitations of human intracranial electroencephalography. Nat. Neurosci. 21, 474–483. https://doi.org/10.1038/ s41593-018-0108-2
- Pascovich, C., Castro-Zaballa, S., Mediano, P.A.M., Bor, D., Canales-Johnson, A., Torterolo, P., Bekinschtein, T.A., 2022. Ketamine and sleep modulate neural complexity dynamics in cats. Eur. J. Neurosci. 55, 1584–1600. https://doi.org. 10.1111/ejn.15646.
- Peyrache, A., Khamassi, M., Benchenane, K., Wiener, S.I., Battaglia, F.P., 2009. Replay of rule-learning related neural patterns in the prefrontal cortex during sleep. Nat. Neurosci. 12, 919–926. https://doi.org/10.1038/nn.2337.
- Pryluk, R., Kfir, Y., Gelbard-Sagiv, H., Fried, I., Paz, R., 2019. A tradeoff in the neural code across regions and species. Cell 176, 597–609.e18. https://doi.org/10.1016/j. cell.2018.12.032.
- Quian Quiroga, R., Panzeri, S., 2009. Extracting information from neuronal populations: information theory and decoding approaches. Nat. Rev. Neurosci. 10, 173–185. https://doi.org/10.1038/nrn2578.
- Rasch, B., Born, J., 2013. About sleep's role in memory. Physiol. Rev. 93, 681–766. https://doi.org/10.1152/physrev.00032.2012.
- Ray, S., Maunsell, J.H.R., 2011. Different origins of gamma rhythm and high-gamma activity in macaque visual cortex. PLOS Biol. 9, e1000610. https://doi.org/10.1371/ journal.pbjo.1000610.
- Rayan, A., Agarwal, A., Samanta, A., Severijnen, E., van der Meij, J., Genzel, L., 2024. Sleep scoring in rodents: criteria, automatic approaches and outstanding issues. Eur. J. Neurosci. 59, 526–553. https://doi.org/10.1111/eip.15884.
- Rechtschaffen, A., Kales, A., 1968. A manual of standardized terminology, techniques and scoring system for sleep stages of human subjects A. In: Rechtschaffen, Kales, A. (Eds.), National Institute of Neurological Diseases and Blindness, Neurological Information. U. S..
- Rich, E.L., Wallis, J.D., 2017. Spatiotemporal dynamics of information encoding revealed in orbitofrontal high-gamma. Nat. Commun. 8, 1139. https://doi.org/10.1038/ s41467-017-01253-5
- Rieke, F., Warland, D., Van Steveninck, R., de, R., Bialek, W., 1999. Spikes: exploring the neural code. MIT press.
- Rothschild, G., Eban, E., Frank, L.M., 2017. A cortical–hippocampal–cortical loop of information processing during memory consolidation. Nat. Neurosci. 20, 251–259. https://doi.org/10.1038/nn.4457.
- Salinsky, M.C., Oken, B.S., Morehead, L., 1994. Intraindividual analysis of antiepileptic drug effects on EEG background rhythms. Electroencephalogr. Clin. Neurophysiol. 90, 186–193. https://doi.org/10.1016/0013-4694(94)90090-6.
- Schabus, M., Gruber, G., Parapatics, S., Sauter, C., Klosch, G., Anderer, P., Klimesch, W., Saletu, B., Zeitlhofer, J., 2004. Sleep spindles and their significance for declarative memory consolidation. Sleep 27, 1479–1485.
- van Schalkwijk, F.J., Weber, J., Hahn, M.A., Lendner, J.D., Inostroza, M., Lin, J.J., Helfrich, R.F., 2023. An evolutionary conserved division-of-labor between archicortical and neocortical ripples organizes information transfer during sleep. Prog. Neurobiol. 227, 102485. https://doi.org/10.1016/j.pneurobio.2023.102485.

- Schonauer, M., Alizadeh, S., Jamalabadi, H., Abraham, A., Pawlizki, A., Gais, S., 2017. Decoding material-specific memory reprocessing during sleep in humans. Nat. Commun. 8, 15404. https://doi.org/10.1038/ncomms15404.
- Schreiner, T., Petzka, M., Staudigl, T., Staresina, B.P., 2021. Endogenous memory reactivation during sleep in humans is clocked by slow oscillation-spindle complexes. Nat. Commun. 12, 3112. https://doi.org/10.1038/s41467-021-23520-2.
- Schreiner, T., Staudigl, T., 2020. Electrophysiological signatures of memory reactivation in humans. Philos. Trans. R. Soc. B Biol. Sci. 375, 20190293. https://doi.org/ 10.1098/rstb.2019.0293.
- Schwartenbeck, P., Baram, A., Liu, Y., Mark, S., Muller, T., Dolan, R., Botvinick, M., Kurth-Nelson, Z., Behrens, T., 2023. Generative replay underlies compositional inference in the hippocampal-prefrontal circuit. Cell 186, 4885–4897.e14. https://doi.org/10.1016/j.cell.2023.09.004.
- Simor, P., van der Wijk, G., Nobili, L., Peigneux, P., 2020. The microstructure of REM sleep: why phasic and tonic? Sleep. Med. Rev. 52, 101305. https://doi.org/10.1016/j.smrv.2020.101305.
- Slama, S.J.K., Jimenez, R., Saha, S., King-Stephens, D., Laxer, K.D., Weber, P.B., Endestad, T., Ivanovic, J., Larsson, P.G., Solbakk, A.-K., et al., 2021. Intracranial recordings demonstrate both cortical and medial temporal lobe engagement in visual search in humans. J. Cogn. Neurosci. 33, 1833–1861. https://doi.org/10.1162/jocn_a01739
- Staresina, B.P., Bergmann, T.O., Bonnefond, M., van der Meij, R., Jensen, O., Deuker, L., Elger, C.E., Axmacher, N., Fell, J., 2015. Hierarchical nesting of slow oscillations, spindles and ripples in the human hippocampus during sleep. Nat. Neurosci. 18, 1679–1686. https://doi.org/10.1038/nn.4119.
- Steiger, J.H., 1980. Tests for comparing elements of a correlation matrix. Psychol. Bull. 87, 245–251. https://doi.org/10.1037/0033-2909.87.2.245.
- Steriade, M., Timofeev, I., Grenier, F., 2001. Natural waking and sleep states: a view from inside neocortical neurons. J. Neurophysiol. 85, 1969–1985. https://doi.org/ 10.1152/in.2001.85.5.1969.
- Timme, N.M., Lapish, C., 2018. A tutorial for information theory in neuroscience. eNeuro 5. https://doi.org/10.1523/ENEURO.0052-18.2018.
- Tononi, G., Cirelli, C., 2014. Sleep and the price of plasticity: from synaptic and cellular homeostasis to memory consolidation and integration. Neuron *81*, 12–34. https://doi.org/10.1016/j.neuron.2013.12.025.
- Treves, A., Panzeri, S., 1995. The upward bias in measures of information derived from limited data samples. Neural Comput. 7, 399–407. https://doi.org/10.1162/ neco.1995.7.2.339.
- Vaz, A.P., Wittig, J.H., Inati, S.K., Zaghloul, K.A., 2020. Replay of cortical spiking sequences during human memory retrieval. Science 367, 1131–1134. https://doi. org/10.1126/science.aba0672.
- Vaz, A.P., Wittig, J.H., Inati, S.K., Zaghloul, K.A., 2023. Backbone spiking sequence as a basis for preplay, replay, and default states in human cortex. Nat. Commun. 14, 4723. https://doi.org/10.1038/s41467-023-40440-5.
- Vyazovskiy, V.V., Delogu, A., 2014. NREM and REM sleep: complementary roles in recovery after wakefulness. Neuroscientist 20, 203–219. https://doi.org/10.1177/ 1073858413518152.
- Watson, B.O., Ding, M., Buzsáki, G., 2018. Temporal coupling of field potentials and action potentials in the neocortex. Eur. J. Neurosci. 48, 2482–2497. https://doi.org/ 10.1111/ein.13807.
- Watson, B.O., Levenstein, D., Greene, J.P., Gelinas, J.N., Buzsáki, G., 2016b. Multi-unit spiking activity recorded from rat frontal cortex (brain regions mPFC, OFC ACC, M2) wake-Sleep. Epis. wherein least 7 Min. wake are Follow. 20 Min. Sleep. CRCNS.org. https://doi.org/10.6080/K02N5060.
- Watson, B.O., Levenstein, D., Greene, J.P., Gelinas, J.N., Buzsáki, G., 2016a. Network homeostasis and state dynamics of neocortical sleep. Neuron 90, 839–852. https:// doi.org/10.1016/j.neuron.2016.03.036.
- Wilber, A.A., Skelin, I., Wu, W., McNaughton, B.L., 2017. Laminar organization of encoding and memory reactivation in the parietal cortex. Neuron 95, 1406–1419.e5. https://doi.org/10.1016/j.neuron.2017.08.033.
- Wilson, M.A., McNaughton, B.L., 1994. Reactivation of hippocampal ensemble memories during sleep. Science 265, 676–679. https://doi.org/10.1126/science.8036517.